DTU Library

Simulation of Wind Farms in Flat & Complex terrain using CFD

Prospathopoulos, John; Cabezon, D.; Politis, E.S.; Chaviaropoulos, P.K.; Rados, K.G.; Schepers, J.C.; Hansen, Kurt Schaldemose; Barthelmie, R.J.

Published in:
Torque 2010

Publication date:
2010

Link back to DTU Orbit

Simulation of Wind Farms in Flat and Complex Terrain using CFD

J. M. Prospathopoulos[1]
jprosp@cres.gr
K. G. Rados[3]
kgrados@teikoz.gr

D. Cabezon[2]
dcabezon@cener.com
J. G. Schepers[4]
schepers@ecn.nl

E. S. Politis[1]
vpolitis@cres.gr
K. Hansen[5]
ksh@mek.dtu.dk

P. K. Chaviaropoulos[1]
tchaviar@cres.gr
R. J. Barthelmie[6]
rbarthel@indiana.edu

[1]: Centre of Renewable Energy Sources and Svaing, Greece
[2]: National Renewable Energy Centre of Spain
[3]: School of Mechanical Engineering, National Technical University of Athens
[4]: Energy Research Centre of the Netherlands
[5]: Department of Mechanical Engineering, Technical University of Denmark
[6]: Atmospheric Science and Sustainability, Department of Geography, Indiana University

Abstract

Use of computational fluid dynamic (CFD) methods to predict the power production from wind entire wind farms in flat and complex terrain is presented in this paper. Two full 3D Navier–Stokes solvers for incompressible flow are employed that incorporate the k–ε and k–ω turbulence models respectively. The wind turbines (W/Ts) are modelled as momentum absorbers by means of their thrust coefficient using the actuator disk approach. The WT thrust is estimated using the wind speed one diameter upstream of the rotor at hub height. An alternative method that employs an induction-factor based concept is also tested. This method features the advantage of not utilizing the wind speed at a specific distance from the rotor disk, which is a doubtful approximation when a W/T is located in the wake of another and/or the terrain is complex. To account for the underestimation of the near wake deficit, a correction is introduced to the turbulence model. The turbulence time scale is bounded using the general "realizability" constraint for the turbulent velocities. Application is made on two wind farms, a five-machine one located in flat terrain and another 43-machine one located in complex terrain. In the flat terrain case, the combination of the induction factor method along with the turbulence correction provides satisfactory results. In the complex terrain case, there are some significant discrepancies with the measurements, which are discussed. In this case, the induction factor method does not provide satisfactory results.

Keywords: Wind turbine wakes, CFD modelling, complex terrain, induction factor, turbulence model correction.

1 Introduction

The ongoing development of wind energy has created the need for installing large wind farms not only in flat terrain, but also in off-shore and complex terrain. The wakes formed downstream of the operating W/Ts in all cases interact with the neighboring W/Ts reducing their power production and increasing the turbulence level and the fluctuating loads on their blades. The interaction of the turbulent W/T wakes with the atmospheric boundary layer constitutes a complicated physical problem, which becomes even more complicated in complex terrain. Since accurately quantifying power losses due to wind turbine wakes is an important part of the overall wind farm economics in conjunction with the need for maximizing the deployment of wind energy is the reason behind the scientific efforts for improving the available prediction methods.

During the last three decades many models have been developed to simulate individual WTs and wind farms and estimate the power production. They comprise the whole range of models from straightforward engineering-type ones up to complete 3D Navier–Stokes solvers, which became eventually popular with the increase in the computing power.

A first systematic evaluation of the performance of several wind farm models in off-shore wind farm environments

occurred in the context of the ENDOW project [1]. Six models of varying complexity were evaluated against experimental data from the Vindeby and Bockstigen wind farms. The simplest approaches were the analytical model developed in the Uppsala University (MIUU) and the semi-analytical model of RISØ [2]. The former one was based on the Taylor hypothesis using the transport time for the wake development [3]. The latter was based on an approximate solution of the boundary layer equations neglecting the pressure term, assuming a axisymmetric wake deficit and adopting a similarity assumption for the shape of the wake deficit. University of Oldenburg (UO) used the FLaP model, an implementation of the wake model proposed by Anslie [4]. It was an axisymmetric model solving the momentum and continuity equations with an eddy-viscosity closure. The wake modelling started at the end of near wake with an empirical profile as boundary condition.

ECN used the WAKEFARM program [5], a slightly modified version of the UPMWAKE program [6], which has been developed by the Universidad Politecnica de Madrid. It was a parabolic CFD method in which the turbulent processes in the far wake were modeled through a k–ε turbulence model. Windfarmer [7], an axisymmetric Navier–Stokes model with eddy-viscosity closure, was used by Garrad-Hassan. This also needed an empirical profile for initiation at a distance of 2 rotor diameters (D) downstream of the rotor. Finally, Robert Gordon University (RGU) used a more advanced model, a CFD fully elliptic turbulent 3D Navier–Stokes solver (3D–NS) with k–ε turbulence closure based on a previous axisymmetric model [3]. The rotor was approximated by means of a semi-permeable disk to simulate the pressure drop across a real rotor disk.

Considerable variability in the predictions of the various models was observed. The largest discrepancy appeared in the near wake region, 3 D and 5 D downwind of the rotor, and showed the importance of the near wake parameterisation for the overall wake model performance. Almost all models overestimated the wake effects at 9.6 D downstream of the rotor in terms of the wind speed deficit and the turbulence intensity levels. The 3D CFD models of ECN and RGU agreed quite well in both the wind speed deficit and the turbulence

intensity profiles, but it was not clear whether they performed better than the simpler models when compared to the measurements with the exception of the turbulence intensity predictions.

Further investigation showed that appears to be a fundamental difference between the behaviour of wakes in small wind farms, where standard models performed adequately [8], and in large multi-row wind farms, where current wind farm models appear to under-predict wake losses [9]. In the small off-shore wind farm of Middelgrunden, which consists of 20 W/Ts in a single bow line, the WAsP wake model that is based on linear expansion of the wake downstream [9] [10] gave satisfactory predictions. On the other hand, in the large off-shore multi-row wind farm of Horns-Rev, the analytical model of Frandsen [12], which applies different relationships on 3 predefined flow regimes as flow is expanding, appeared to under-predict wake losses at large distances.

In the context of the on-going EC-funded UpWind project, it was attempted to evaluate and improve the existing wake/wind farm models through comparison with data from large (multi-row) offshore and onshore wind farms. An assessment of the existing wind farm models was carried out using experimental data from the Danish offshore wind farm Horns Rev [13]. Models of varying complexity were tested starting from the straightforward WAsP model [14] and reaching to complete 3D Navier–Stokes solvers. The WindFarmer [7], and the WAKEFARM [5] models also participated in the comparisons along with full 3D Navier–Stokes solvers [1] models that employ the actuator disk method for the thrust calculation.

Predictions of the normalized power of the W/Ts were compared with measurements for the wind direction of 270° for various sector widths, in the range of $\pm1^{o}$ to $\pm15^{o}$. The results revealed that the CFD models over-predict the wake losses in the narrow sectors, while the simpler wind farm models tend to under-predict wake losses, unless their coefficients are calibrated to match the observations. As in ENDOW project, a thorough assessment turned out to be difficult in the comparisons attempted within the UpWind project due to the large uncertainties associated with the measured data, and can be partly attributed to the atmospheric conditions.

The present paper includes the findings from the work carried out within the context of the UpWind project, and its related to complex terrain. Two full 3D Navier–Stokes solvers for incompressible flow are utilized to model entire wind farms in flat and complex terrain. The two solvers, referred to as CFDWake (employed by CENER and is based on commercial code Fluent 6.3) and Cres–flowNS (developed in CRES) use the k–ε and k–ω turbulence models, respectively. W/Ts are modelled as momentum absorbers by means of their thrust coefficient.

The aim of the work is, first to address and investigate a couple of issues still present in wind farms, and second to evaluate two advanced CFD models against existing measurements in a large wind farm located in complex terrain, where simpler models cannot be applied.

2 Description of models

2.1 CRES–flowNS

CRES–flowNS [15] is a full 3D Navier-Stokes solver with a k-ω turbulence closure, suitably modified for neutral atmospheric conditions. The momentum equations are numerically integrated introducing a matrix-free pressure correction algorithm which maintains the compatibility of the velocity and pressure field corrections. Discretization is performed with the finite volume technique using a body-fitted coordinate transformation on a curvilinear mesh. Convection terns are handled by a second order upwind scheme bounded through a limiter, whereas centred second order schemes are employed for the diffusion terms. Velocity-pressure decoupling is prevented by a linear fourth order dissipation term added into the continuity equation.

The modified constants for neutral atmospheric conditions, according to [16], of the standard k–ω turbulence model are:

$$\alpha = 0.3706, \quad \beta = 0.0275, \quad \beta_* = 0.033,$$
$$\sigma = 0.5, \quad \sigma_* = 0.5 \tag{1}$$

For stable atmospheric conditions, the following production term is added to the k equation that accounts for the buoyancy effect [17]:

$$G = -\mu_t \left(\frac{\partial U}{\partial z} \right)^2 \cdot \frac{Ri}{f_m}, \tag{2}$$

where the Richardson number, Ri, is estimated as [18]:

$$Ri = \zeta \frac{0.74 + 4.7\zeta}{1 + 4.7\zeta^{\,2}} \tag{3}$$

and $f_m = 1 + 5\zeta$ with $\zeta = z / L$. The Monin-Obukhov length, L, characterizes the degree of stability.

2.2 CFDWake

CFDWake is an elliptic CFD wake model [19] based on the coupling between the actuator disk technique and CFD wind modelling, implemented through the commercial software package FLUENT. Once the grid is generated, the steady state 3D Navier–Stokes equations are solved: the continuity equation, the three momentum equations and the transport equations for k and ε. A second-order upwind discretization scheme based on multilinear reconstruction approach is used for all dependent variables The standard k–ε turbulence model is used with modified constants adapted to the features of the surface boundary layer [20]:

$$C_{1\varepsilon} = 1.176, \quad C_{2\varepsilon} = 1.92, \quad C_\mu = 0.033,$$
$$\sigma = 1.0, \quad \sigma_* = 1.3 \tag{4}$$

2.3 Boundary conditions

Both models use the vertical profiles of the fully developed turbulent surface boundary layer as free-stream conditions at the inlet of the computational domain [20]. The inflow wind speed profile follows the logarithmic law:

$$U_x = \frac{u_*}{K} \left[ln\,z / z_0\ + c\ z \right] \tag{5}$$

with $c(z) = 0$ and $c(z) = 5z / L$ for neutral and stable conditions, respectively. u_* stands for the friction velocity in Eq. (5), K is the von-Karman constant and z_0 is the roughness length. The inflow profile of k is given by the relationship [18]:

$$k = \frac{u_*^2}{\sqrt{\beta_*}} \cdot \left(\frac{f_\omega}{f_m} \right)^{0.5} \tag{6}$$

where $\beta_* = C_\mu = 0.033$. The respective profiles for ω and ε are:

$$\omega = \frac{u}{\sqrt{\beta_*} \cdot K \cdot z}\ f_\omega \cdot f_m^{\;0.5}, \quad \varepsilon = \frac{u_*^3}{K \cdot z} f_\omega \tag{7}$$

$f_m = f_\omega = 1$ in neutral conditions. In stable conditions $f_m = 1 + 5\zeta$ and $f_\omega = 1 + 4\zeta$.

Neumann conditions (zero gradients) are imposed for all quantities at the top and lateral boundaries. At the outlet, CRES–flowNS also applies Neumann conditions, whereas CFDWake equals the pressure to its atmospheric value. Both codes use wall functions close to the ground. CRES–flowNS demands that the logarithmic profile of Eq. (5) is maintained at the first grid point above ground. CFDWake adapts the standard wall functions by setting a link between the turbulent law of the wall modified for mechanical roughness and the surface boundary layer log-law based on the roughness length.

2.4 Thrust estimation

Both models consider the rotor disks of the wind turbines as momentum absorbers upon which a uniform distribution of axial forces is applied. The axial force that the wind turbines exert over the incoming flow is prescribed from the linear momentum theory and it is calculated through the thrust coefficient for a corresponding upstream wind speed:

$$F = 0.5\rho\, U_{ref}^2\, C_T\, A \qquad (8)$$

where ρ is the air density, U_{ref} is the reference velocity for the thrust coefficient calculation, $C_T = C_T(U_{ref})$ is the thrust coefficient and A is the surface area of the rotor disk. The rotor disk of each W/T is discretized by a number of control volumes. Each control volume acts as a momentum sink through the actuator force estimate by Eq, (8).

In flat terrain cases, the rotor disks of the W/Ts are perpendicular to the main flow and they lie on the y-z planes of the computational grid. However, in complex terrain, the discretization of the rotor disks must be done taking into account the fact that the orientation of the W/T rotors may not be perpendicular to the main flow direction. To this end, CRES–flowNS performs a first computation without W/Ts (including only the terrain topography) to estimate the yaw angle at each rotor disk. Assuming operation with no yaw misalignment, the predicted wind direction at the hub height gives each W/T's orientation. Next, the discretization of the rotor disks is carried out using the grid cells that fulfill certain geometrical criteria regarding the W/T's orientation and the distance from the ground.

Stemming from the definition of the thrust coefficient from single W/T operation in flat terrain and uniform conditions, it is common practice to use the wind speed 1 D upwind of the rotor, either at hub height or averaging over the rotor disk area, for the estimation of the thrust. Therefore, such an approximation can be considered as valid only in cases that the flow field upstream of the W/T is not affected by the terrain and/or by the wakes of upstream or neighbouring W/Ts. On the contrary, in cases of complex terrain or multi-wake interactions even in flat terrain, the definition of the reference wind speed is not obvious.

To ameliorate this methodological pitfall, another alternative is implemented in CRES–flowNS method that is based on the definition of the induction factor:

$$a = \frac{U_{ref} - U_{disk}}{U_{ref}} \qquad (9)$$

where U_{ref} is the, unknown, W/T reference wind speed and U_{disk} is the wind speed at hub height or the average wind speed over the disk surface. In addition, the W/T thrust coefficient can be expressed as a function of the induction factor [21]:

$$C_T = \begin{cases} 4a\,(1-a)\,, & a < 0.4 \\ 0.89 - \dfrac{0.20 - (a - 0.143)^2}{0.643}, & a \geq 0.4 \end{cases} \qquad (10)$$

Eqs. (9) and (10) along with the thrust coefficient curve $C_T = C_T(U_{ref})$ can be solved iteratively to provide the U_{ref} value. This method has the advantage that the estimation of U_{ref} is not linked to the determination of a certain distance upstream of the W/T. However, it bears potential and uniform flow approximations that are inherent in the induction factor relationships employed.

On the other hand, CFDWake utilizes another approach, according to which, the model is first calibrated for the free-stream conditions on the reference wind turbine and then the momentum absorbers representing the WT rotors are activated in a sequential manner from the first up to the last row: First, a run is performed without W/Ts to estimate the free stream wind speed values at the W/T positions (hub height) in the first row. These values are used to prescribe the corresponding sink terms according to Eq. (8), in a second run, including only the first row of W/Ts, The resulting wind speeds at the positions of the W/Ts in the second row

are then used as the reference wind sped and the corresponding sink terms are estimated and activated in a third run, which includes the first and second row of W/Ts. This process is made until the last row is reached. In this way, the simulation operates in a hybrid parabolic-elliptic mode. It is obvious that this approach can be effectively applied only in cases that the flow is nearly perpendicular to the rows of W/Ts, since in any other cases it would require a number of steps equal to the number of the WT in the wind farm.

2.5 Turbulence correction

A significant underestimation of the near wake deficit has been reported in W/T simulations, especially in neutral atmospheric conditions. El Kasmi and Masson [22] attributed the wake deficit underestimation to the existence of a non-equilibrium region close to the turbine, where an enhancement of the rate of turbulence dissipation occurs. Based on that, several alternatives have been suggested to delay the wake flow recovery [23]. However, their main deficiency is the dependence upon constants that need tuning with experimental data.

According to Réthoré [24] the reason of wake deficit underestimation is that two-equation turbulence models predict a too high normal Reynolds stress in the area surrounding the wind turbine leading to a large growth of turbulent kinetic energy. The assumptions of velocity conservation during the turbulent time scale, as well as the linearity of the mean velocity field over the turbulent length scale are not valid in the whole region of the near wake.

To ameliorate this anomaly, a concept already applied in stagnation point aerodynamic flows [25], where a similar behavior of the two-equation turbulence models has been observed is introduced in CRES–flowNS. It is based on the "realizability" constraint $2k \geq \overline{u^2} \geq 0$, where u can be any component of the fluctuating velocity. By applying this constraint on the eddy-viscosity formula written in the principal axes of the strain tensor, the following bound for the turbulent time scale is obtained:

$$T = min\left(\frac{1}{\omega}, \frac{2}{3}\sqrt{\frac{3}{8S^2}}\right), \qquad (11)$$

where $S^2 = S_{ij} \cdot S_{ji}$ and S_{ij} is the strain tensor given by the relationship:

$$S_{ij} = \frac{1}{2}\left(\frac{\partial U_i}{\partial x_j} + \frac{\partial U_j}{\partial x_i}\right) \qquad (12)$$

with x_i the Cartesian coordinates and U_i being the velocity components. Eq. (11) can be used to substitute the turbulent time scale in the calculation of the turbulent viscosity and the ω transport equation. Due to its general assumptions, this constraint can be applied to any flow simulation, such as atmospheric flows. It has the advantage of not including any parameter that needs tuning.

3 Application to wind farms

3.1 Flat terrain – 5W/Ts in a row

The first application deals with the ECN test farm [26] where 5 W/Ts, denoted as t5, t6, t7, t8 and t9 (with the respective power productions denoted as P5, P6, P7, P8 and P9) are positioned in a row in flat terrain. The diameter and the hub height of the W/Ts are 80 m, while the distance between two successive W/Ts is 3.8 D. Calculations with the CRES–flowNS method are performed for stable conditions in a range of wind directions from -30° to +30°, where 0° refer to the direction of the W/Ts' row.

The computational domain is extended 20 D downstream of the last W/T in the axial direction and 10 D off the rotor planes in the lateral direction. In this way, the flow is not restricted by the computational boundaries, where Neumann conditions are imposed. For each wind direction, the coordinate system is selected so that its origin coincides with the position of the first W/T and the x- axis is aligned with the wind direction. The grid spacing is kept uniform, close to 0.05 D, between the W/Ts, and increases downstream of the last W/T, following a geometrical progression, until the maximum dimension of the domain is reached. In Figure 1 and Figure 2, the generated meshes in the xy-plane are depicted for the 0° and 30° cases.

In the vertical direction, the first three grid-surfaces are positioned close to the ground at heights of 0.01, 0.03 and 0.05 D, respectively. An equidistant fine mesh is constructed over the rotor disk areas using 21 grid points across the rotor diameter. This number of grid points was found to be sufficient after checking the
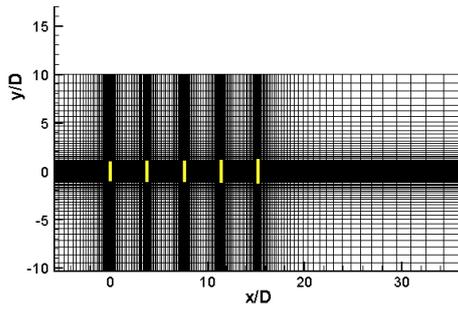
dependency of the predictions for the 0° wind direction.

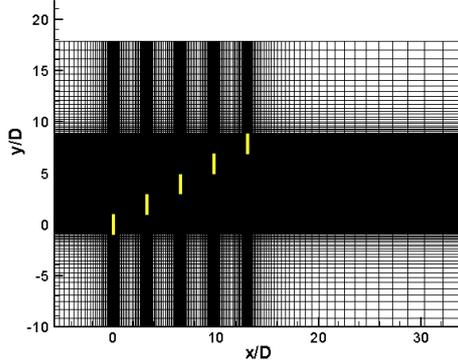Figure 1: Two-dimensional layout of the generated grid for the simulation of the ECN test farm for 0° wind direction.

Figure 2: Two-dimensional layout of the generated grid for the simulation of the ECN test farm for 30° wind direction.

The relative power performances for all W/Ts are first predicted using the baseline simulation which utilizes the average wind speed value 1 D upstream of the rotor plane as reference for the thrust estimation. No correction of the turbulence model is included in this simulation. The fact that the predictions plotted in Figure 3 agree satisfactorily with measurements is not consistent with the expected over-prediction, reported in single wake simulations [22]. In addition, the under-performance of the second W/T, observed in the measurements, is not reflected in the numerical predictions.

Next, the two modelling alternatives are applied to assess their influence on the predictions. First, the reference wind speed for thrust estimation is calculated using the induction factor method. In the predictions plotted in Figure 4, the relative performances have been increased over-estimating the measurements, in accordance with the single wake predictions using two-equation turbulence models.
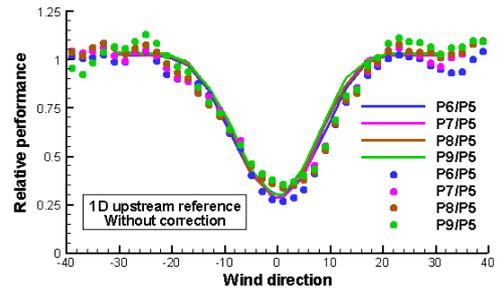

Figure 3: Relative power performances for the ECN test farm (U=6–8m/s). The reference wind speed is defined 1D upstream of the rotor. Lines correspond to predictions, symbols to measurements.
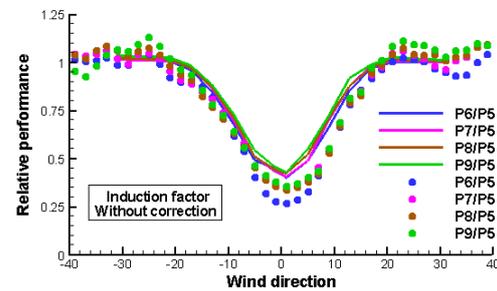

Figure 4: Relative power performances for the ECN test farm (U=6–8m/s). The reference velocity is defined using the induction factor concept. Lines correspond to predictions, symbols to measurements.

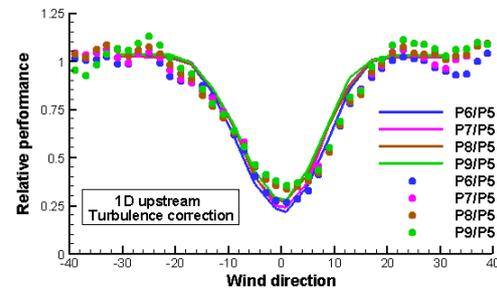
Figure 5: Relative power performances for the ECN test farm (U=6–8m/s). The reference wind speed is defined 1 D upstream of the rotor. Correction of the turbulence model is applied.

The second modeling approach is the correction of the turbulence model. As expected, this restricts the growth of turbulent kinetic energy in the near wake region, increasing the predicted velocity deficit. This effect is depicted in Figure 5. In the same figure, it also observed a slight under-performance of the second W/T, but it is less than what is observed in the measurements.
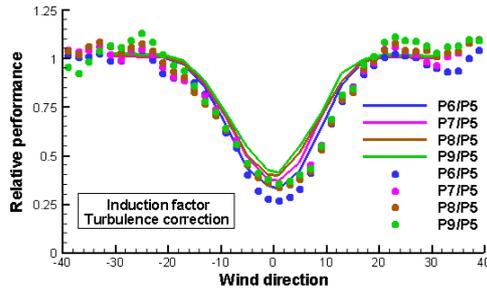
Figure 6: Relative power performances for the ECN test farm (U=6–8m/s). The reference wind speed is defined using the induction factor concept. Correction of the turbulence model is applied.

As a final step, the combination of the two modeling alternatives is applied and the results are shown in Figure 6. The overestimation of the W/Ts' performance has been partially corrected and the under-performance of the second W/T, observed in the experimental data, is reproduced by the calculation.

3.2 Complex terrain – 43W/Ts

Both CRES–flowNS and CFDWake models are applied to a large wind farm located in complex terrain in Spain, with 43 machines positioned in five nearly parallel rows (see Figure 7). The distance between the first 3 rows is about 11 D, whereas the fourth and fifth rows are located farther, at distances 15 D and 22 D from the third row respectively. The distance between two machines in the same row is 1.5 D. It is important to state that 10 out of the 43 machines feature a 10-meter higher hub height than the others.
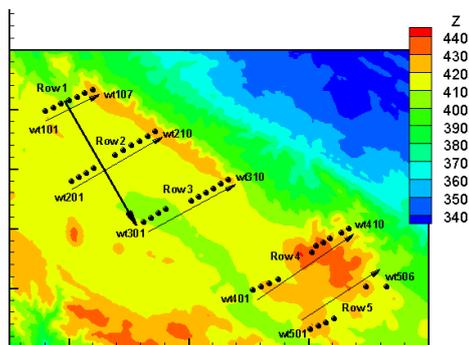

Figure 7: Layout of the complex terrain wind farm. The contours indicate the terrain elevation. The arrow perpendicular to the W/T rows shows the wind direction of 327° that is examined in the paper.

The terrain contours and a layout of the surface grid for the examined case, corresponding to a wind direction value of 327°, are presented in Figure 7 and Figure 8. Figure 7 shows that the main flow direction is almost perpendicular to the W/T rows.
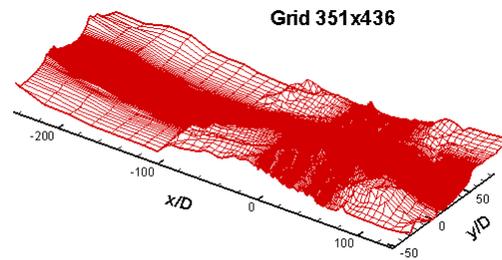

Figure 8: Layout of the surface grid for the wind direction 327° case.

The discretized terrain consists of 351x435 points. Taking into account that 45 grid lines have been used in the vertical direction, the computational grid consists of nearly 7 million grid points. As depicted by Figure 8, the inflow boundary of the computational domain has been placed far enough from the locations of the W/Ts, so that the largest possible part of terrain influencing the development of the flow is taken into account. The grid spacing in the x-y plane starts from a minimum value of 0.1 D at the locations of W/Ts and increases outwards using a geometrical progression.

The measurements refer to neutral atmospheric conditions and they have been collected to correspond to a free stream wind speed of 8 m/s for the first W/T in the first row, which is the reference turbine for power normalization, denoted with wt101 in Figure 7. The actual power productions are averaged from data covering the range 327°±5° of wind direction for the reference W/T. The uncertainties associated to the measured signals are large since the documentation of the signal calibration has been missing during 5 years. The uncertainty is associated to the primary instruments, which need to be calibrated annually if they are used for power curve determination according to standard methods. As a result large standard deviations from the mean value of the measurements have been estimated.

In Figure 9–Figure 12, three sets of predictions using the CRES–flowNS code are depicted. The "no wakes" distributions refer to the predictions without W/Ts that include only the effect of the topography (including and the effect of the different hub height in some WTs), whilst the "flat

terrain" distributions refer to the predictions of the same W/T configuration in flat terrain. In this way, the topography and the wake induced effects are distinguished and can be independently assessed and compared to the power predictions for the complete simulations (denoted as "terrain+wakes" in the figures). Calculations have been performed using the wind speed at hub height 1 D upstream of the W/T as reference value in the thrust estimation.
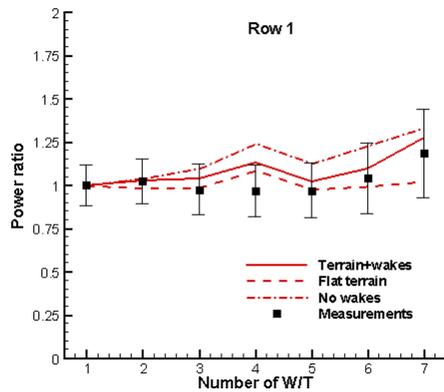

Figure 9: Power ratios of the WTs in the first row, with reference to the first W/T of the same row, for the complex terrain wind farm for wind direction 327°. Terrain and wake effects are distinguished.
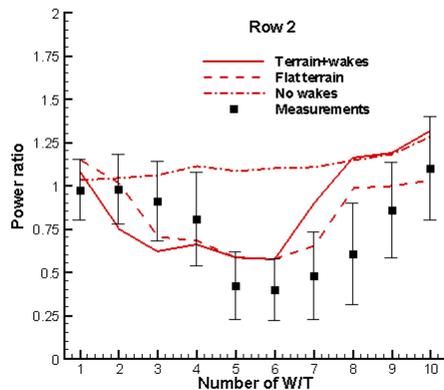

Figure 10: Power ratios of the WTs in the second row, with reference to the first W/T of the first row, for the complex terrain wind farm for wind direction 327°. Terrain and wake effects are distinguished.

The power reduction for most of the wind turbines at the second and third row comes from the interaction with the upstream W/Ts due to the wake effects; however, it seems that the presence of the terrain reduces the wake effect of the preceding W/Ts. At the fourth row, the second group of six W/Ts is not significantly affected by wakes of the preceding turbines, because they are located almost outside of the area that the wakes develop. In addition, they are located at higher terrain altitudes where the topography effect is dominant.
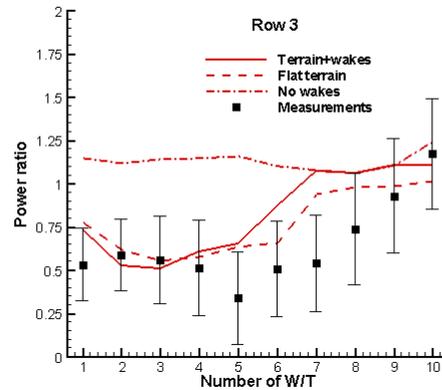

Figure 11: Power ratios of the WTs in the third row, with reference to the first W/T of the first row, for the complex terrain wind farm for wind direction 327°. Terrain and wake effects are distinguished.

Figure 12: Power ratios of the WTs in the fourth row, with reference to the first W/T of the first row, for the complex terrain wind farm for wind direction 327°. Terrain and wake effects are distinguished.
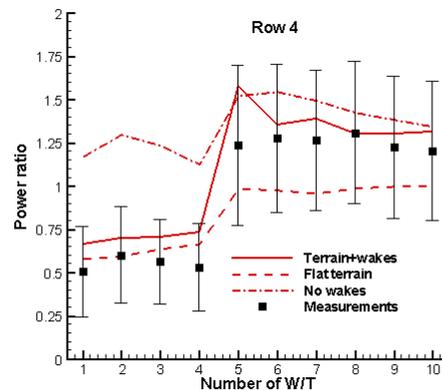
Significant deviations from the measurements are observed for the second group of W/Ts at the second and third row. Possible reasons could be: (a) an erroneous estimation of the reference velocity for thrust calculation, (b) insufficient terrain discretization and (c) the large uncertainty of the experimental data. Regarding (b) it should be noted that grid independency was achieved for the grid density over the rotor disk surfaces (100 grid points proved to be sufficient for grid independent predictions), however, it was not completely achieved for the grid

density for terrain discretization due to the existing computational capabilities.

In Figure 13–Figure 16, the predictions of the CRES–flowNS and CFDWake codes are compared with the measurements. Three sets of CRES–flowNS predictions are presented: The first and second refer to the utilization of the wind speed 1 D upstream of the rotor at hub height for thrust estimation and the third refers to the utilization of the induction factor method for thrust estimation. The second set of predictions resulted using a refined grid for the discretization of the region that includes only the first 3 rows of W/Ts.
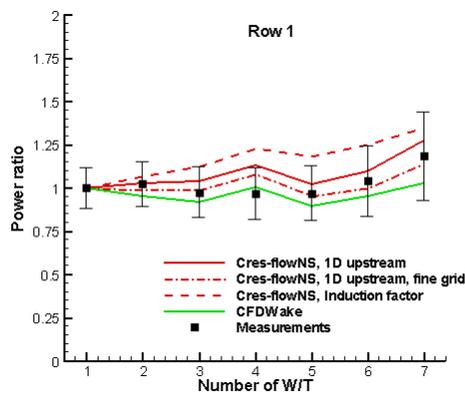

Figure 13: Power ratios of the WTs in the first row, with reference to the first W/T of the same row, for the complex terrain wind farm for wind direction 327°. CRES–flowNS and CFDWake predictions are compared with measurements.
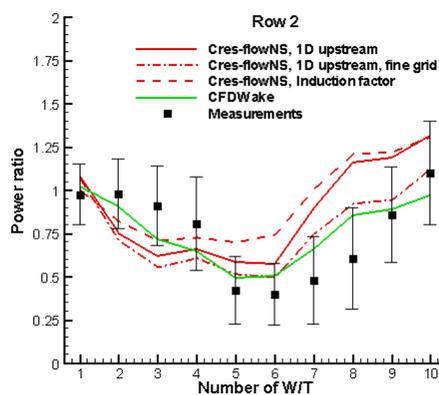

Figure 14: Power ratios of the WTs in the second row, with reference to the first W/T of the first row, for the complex terrain wind farm for wind direction 327°. CRES–flowNS and CFDWake predictions are compared with measurements.

For the same grid density, the predictions using CFDWake exhibit a better

agreement with measurements, with the exception of the second group of W/Ts in the fourth row. This is attributed to the more precise way of thrust estimation, which calculates the reference velocity separately for each row of W/Ts, taking into account the effect of the preceding W/Ts. The predictions of CRES–flowNS are improved when the refined grid is used for the discretization of the terrain, indicating the significance of grid density in complex terrain simulations. On the other hand, the induction factor method significantly over-predicts the power ratios at the second – fourth row, indicating that its use in complex terrain should be further investigated.
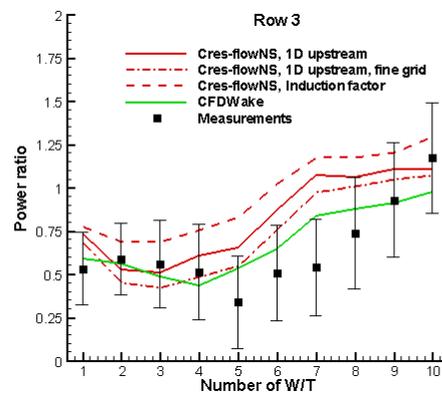

Figure 15: Power ratios of the WTs in the third row, with reference to the first W/T of the first row, for the complex terrain wind farm for wind direction 327°. CRES–flowNS and CFDWake predictions are compared with measurements.
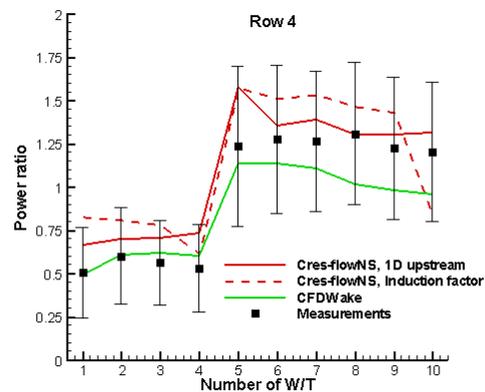

Figure 16: Power ratios of the WTs in the fourth row, with reference to the first W/T of the first row, for the complex terrain wind farm for wind direction 327°. CRES–flowNS and CFDWake predictions are compared with measurements.

It should be noted that the near wake correction has been included in all calculations performed by CRES–flowNS, however, it was found that it does not influence the predictions significantly because of the large distance between the W/Ts (11 D or more).

4 Conclusions

Two full 3D Navier–Stokes models, CRES–flowNS and CFDWake, were applied for the prediction of wind farm performances in flat and complex terrain. Different methods for the thrust estimation of the W/Ts were implemented. In CRES–flowNS the reference wind speed required for the thrust calculation was estimated using two alternatives. In the first one the wind speed at 1 D upstream of the rotor disk was used, while the second one was based on the induction factor concept. The latter has the advantage of not linking the reference wind speed with a specific location upstream the W/T. On the other hand, in CFDWake method thrust was estimated by means of a parabolic method that can be effectively applied only in cases where the W/T rows are nearly parallel to the main flow direction. According to this, a number of sequential runs is performed. Each run provides the reference wind speeds at the W/T positions of the next row by activating the momentum absorbers that represent the wind turbine rotors of the preceding rows. In this way, an accurate determination of the W/T reference wind speed is achieved.

In addition, CRES–flowNS employs a turbulence correction in order to ameliorate the underestimation of near wake deficit by the two-equation turbulence model.

Combination of the induction factor method with the turbulence correction produced satisfactory results in the ECN wind farm comprising 5 W/Ts in a row in flat terrain. However, the same combination was not efficient for a large wind farm in complex terrain where the induction factor method led to an overestimation of the W/T power performances. Better results were produced in this case using as reference wind speed the wind speed value 1 D upstream of the rotor disk at hub height. Using the same grid size in the complex terrain case, CFDWake's predictions were in a closer agreement with measurements,

possibly because of the more accurate determination of the reference velocities for thrust estimation. The predictions of CRES–flowNS were improved when a refined grid was utilized for the terrain discretization, indicating the importance of grid size in complex terrain simulations.

It should be mentioned though, that there was high uncertainty of the measurements in the complex terrain case, related mainly to the calibration of the instruments. The primary uncertainty contributions were associated to the quality of power signals, the wind turbine status signals, the dual rotor speed operation, the quality of nacelle wind speed, the operational quality of the wind turbines, the quality of measured wind speed and direction, the different hub heights of 45 or 55 m represented in the wind farm, the yaw position signals (the offset varies in time) and the turbine yaw misalignment during operation.

References

[1] Rados, K., Larsen, G., Barthelmie, R., Schlez, W., Lange, B., Schepers, G., Hegberg, T., and Magnusson, M., "Comparison of Wake Models with Data for Offshore Windfarms", *Wind Engineering,* 2001, 25(5), pp.271-280

[2] Barthelmie, R.J., et al., "Efficient Development of Offshore Windfarms: a new project for investigating wake and boundary-layer interactions", EWEC 2001, Copenhagen.

[3] Magnusson, M., Rados, K.G., and Voutsinas, S.G., " A study of the flow downstream of a wind turbine using measurements and simulations", *Wind Engineering,* 1996, 20(2), pp.389-403.

[4] Ainslie, J., "Calculating the flow field in the wake of wind turbines", *J. Wind Eng Ind Aerodyn*, 1988, 27, pp.213-224.

[5] Schepers, J.G., "ENDOW: Validation and improvement of ECN's wake model", 2003, ECN-C-03-034.

[6] Crespo, A., Hernandez, J., Fraga, E., Andreu, C., "Experimental validation of the UPM computer code to calculate wind turbine wakes and comparison with other models", *J. Wind Eng Indl Aerodyn*, 1988, 27, pp. 77-88

[7] Schlez, W., Neubert, A., Smith, G., "New Developments in Precision Wind Farm Modelling, DEWEK 2006, Bremen, Germany.

[8] Barthelmie, R.J., Frandsen, S.T., Nielsen, M.N., Pryor, S.C., Rethore, P.-E., Jørgensen, H.E, "Modelling and measurements of power losses and turbulence intensity in wind turbine wakes at Middelgrunden offshore wind farm", *Wind Energy*, 2007, 10, pp.517-528.

[9] Mechali, M., Jensen, L., Barthelmie, R., Frandsen, S., and Rethore, P.E., "Wake effects at Horns Rev and their influence on energy production", in Proceedings of European Wind Energy Conference and Exhibition, 2006, p.10, Athens, Greece.

[10] Jensen, N.O., "A note on wind turbine interaction", 1983, Risø National Laboratory, Roskilde, Denmark, 16, Risø-M-2411.

[11] Katic, I., Højstrup, J., Jensen. N.O., " A simple model for cluster efficiency", *European Wind Energy Association*, Rome, 1986, pp.407-409.

[12] Frandsen, S., Barthelmie, R., Pryor, S., Rathmann, O., Larsen. S., Højstrup., J., Thøgersen, M., "Analytical modelling of wind speed deficit in large offshore wind farms", *Wind Energy*, 2006, 9, pp.39-53.

[13] Barthelmie, R.J., Hansen, K, Frandsen, S.T., Rathmann, O., Schepers, J.G., Schlez, W., Phillips, J., Rados, K., Zervos, A., Politis, E.S., and Chaviaropoulos, P.K., "Modelling and Measuring Flow and Wind Turbine Wakes in Large Wind Farms Offshore", *Wind Energy*, 2009, 12(5), pp. 431-444.

[14] Troen, I., Petersen, E.L., *European Wind Atlas*, Risø National Laboratory, Roskilde, Denmark, 1989:656

[15] Chaviaropoulos, P.K. and Douvikas, D.I., "Mean-flow-field Simulations over Complex Terrain Using a 3D Reynolds Averaged Navier–Stokes Solver," *Proceedings of ECCOMAS '98*, 1998, 1(2), pp. 842-848

[16] Prospathopoulos, J.M., Politis, E.S., Chaviaropoulos, P.K., "Modelling wind turbines in complex terrain", Proceedings of the 2008 European Wind Energy Conference & Exhibition, Brussels

[17] Stull, R. B., *An introduction to boundary layer meteorology*, ISBN 90-277-2768-6 ed. Kluwer Publications Ltd, 1988

[18] Panofsky, H., Dutton, J., *Atmospheric Turbulence*, Wiley, New York, 1984

[19] Cabezón D., Sanz J., Martí I., Crespo A., "CFD modelling of the interaction between the Surface Boundary Layer and rotor wake. Comparison of results obtained with different turbulence models and mesh strategies", In Proceeding of EWEC 2009, Marseille, France, March 2009

[20] Sanz J., Cabezón D., Martí I., Patilla P., van Beeck J., "Numerical CFD modelling of non-neutral atmospheric boundary layers for offshore wind resource assessment based on Monin-Obukhov theory", In Proceedings of EWEC 2008, Brussels, Belgium, April 2008

[21] Eggleston, D.M., and Stoddard, F.S., *Wind Turbine Engineering Design*, Van Nostrand Reinhold, New York, 1987, pp. 30–35, 58.

[22] El Kasmi, A., and Masson, C., "An extended k-ε model for turbulent flow through horizontal axis wind turbines", J. of Wind Eng. Ind. Aerodyn., 2008, 96, pp.103-122.

[23] Politis, E.S., Rados, K., Prospathopoulos, J., Chaviaropoulos, P.K., Zervos, A., "CFD modeling issues of wind turbine wakes under stable atmospheric conditions", EWEC '09, Marseille, France, March 16-19, 2009.

[24] Réthoré, P-E, Sorensen, N.N., "Turbulence Closure Strategies for Modelling Wind Turbines Wake in Atmospheric Turbulence", Euromech

Colloquium 508, October 2009, Madrid.

[25] Durbin, P.A., "On the k-ε stagnation point anomaly", *Int. J. Heat and Fluid Flow*, 1996, 17(1), pp.89-90.

[26] Machielse, L.A.H., Eecen, P.J., Korterink, H., van der Pijl, S.P. and Schepers, J.G., "ECN Test Farm Measurements For Validation of Wake Models", Proceedings of the 2007 European Wind Energy Conference & Exhibition, Milan 7-10/5/2007, Edited by P. K. Chaviaropoulos, pp. 98-102.